

Heat Capacity of PuO₂ at High Temperature: a Comparison of Interatomic Potentials

Rolando Calabrese

ENEA

Via Martiri di Monte Sole, 4

37129, Bologna, Italy

rolando.calabrese@enea.it

ABSTRACT

The design of mixed oxide fuel (MOX) for fast breeder reactors (FBR) foresees concentrations of PuO₂ of the order of 30 mol%. The radial redistribution of actinides occurring under irradiation brings to local concentrations of plutonium higher than those considered in fresh fuel. Therefore, a careful verification of the effect of plutonium concentration on fuel properties such as thermal conductivity, melting temperature, thermal creep is mandatory for both safety reasons and economic reasons. Heat capacity is relevant for thermal conductivity and behaviour under transient conditions. There is a straightforward correlation between MOX heat capacity and PuO₂ heat capacity that is expressed by means of the Neumann-Kopp rule (NK). A lack of measurements at high temperature has prevented an accurate modelling of plutonium dioxide heat capacity. If on the one hand, in past reviews it has been recommended a nearly flat behaviour up to the melting temperature, on the other hand, more recent models assume that a significant increase of heat capacity occurs at high temperature with values higher than UO₂. In our previous MD calculations we have discussed the heat capacity of PuO₂ at high temperature by comparing the results of two interatomic potentials. A critical review has confirmed that some aspects of these results required a deeper consideration. The paper presents changes introduced in modelling descending from the outcomes of our review. In the light of this revised modelling, new MD calculations have in general confirmed our previous conclusions. Besides this, results on the Grüneisen constant and Bulk modulus are presented.

1 INTRODUCTION

The thermophysical properties of PuO₂ are relevant for fast reactor MOX fuel where concentrations of plutonium dioxide up to 30 mol% are considered [1,2]. Actinides redistribution occurring under irradiation leads to local concentrations of plutonium much higher than the nominal value [3]. For these reasons the impact of plutonium concentration on MOX fuel performance must be carefully studied. In this frame, a lack of experimental measurements has raised questions on the heat capacity of PuO₂ in the temperature interval extending from 2400 K up to the melting temperature. As a consequence, a significant scatter of models' predictions is noticed in this temperature region. Some authors have proposed a two-term model that is sufficient to accurately predict existing experimental measurements of heat capacity [4-6]. In this case contributions to the heat capacity of PuO₂ come from the phonon and dilation terms. In these models, based on the hypothesis that excess heat capacity is due to electronic disorder and that PuO₂ is a semiconductor material, the term accounting for the formation of defects is neglected [4-6]. Other authors have assumed that the formation of oxygen Frenkel pair (OFP) defects leads to a significant increase of PuO₂ heat capacity

[7,8]. Recent recommendations [9] and modelling [2] have been developed in agreement with the correlation proposed in [8]. Together with the topic of excess heat capacity, also the presence of the Bredig transition has been debated in the open literature. This transition that is revealed by a peak of heat capacity around 85% of the melting temperature has been predicted in [7,10]. Models and experimental data have not confirmed the presence of a superionic transition [10,11]. Author has carried out MD calculations on the heat capacity of PuO₂ [12]. Outcomes of this analysis confirmed an increase of heat capacity at high temperature occurring beyond 85% of the melting temperature. These results were not in agreement with the presence of a peak of heat capacity. An effect due to the formation energy of OFP was confirmed as well as that clustering and coupling of defects play a major role. A critical review performed by the author on the results presented in [12] has revealed some aspects requiring a more detailed analysis. These issues concern the modelling of heat capacity, the value used for the Grüneisen constant, and the predictions on the linear thermal expansion. Descending from this analysis, modelling has been revised and new MD calculations have been performed. Conclusions drawn in [12] have been reconsidered in the light of the updated results presented here. The model used for the heat capacity has allowed us to make additional calculations on the Grüneisen constant and Bulk modulus of plutonium dioxide as a function of temperature. MD calculations have been performed by means of LAMMPS [13]. Code runs have been carried out on the CRESCO6 cluster [14]. This machine supports the MPI message-passing library giving the opportunity to take advantage of the built-in parallel structure of the code.

2 METHODOLOGY

The review above mentioned has showed that an increase of heat capacity at high temperature was noticed in the results of the defects formation term as well as in the results of the dilation term [12]. This observation has suggested that the increase of heat capacity due to the pre-melting transition shouldn't be shared between different terms for a better interpretation of the phenomenon. A second observation was raised from the deviations seen between the thermal expansion predicted in our calculations and the recommended curve. The third issue under consideration was the use of a value of the Grüneisen constant (1.62) that was defined according to the indications in the open literature [12]. In this case, the value adopted in calculations was lower than recent measurements [15] and its use not well justified. These observations have suggested a refinement of the interatomic potential and a redefinition of the modelling of heat capacity. These two aspects together with a brief description of the correlations and meaning of terms used in MD calculations are presented in following sub-sections.

2.1 Interatomic potentials

Models employed in our MD calculations are based on a Born–Mayer–Huggins (BMH) potential partially ionic with a covalent contribution that is implemented by means of a Morse potential [11,16]. The BMH potential is presented in Eq. 1. Each term of Eq. 1 accounts for different types of interactions between ions: the first for long-range Coulombic; the second and the third for short-range interactions due to Pauli's repulsion principle and van der Waals forces, respectively. Values of effective electronic charges z_i and z_j determine the ionicity of potential; r_{ij} stands for the distance between ion i and ion j . Coefficients of the interatomic potential A_{ij} , ρ_{ij} , and C_{ij} are defined for each couple of interacting ions that is O-O, Pu-Pu, Pu-O.

$$U_{ij}(r_{ij}) = \frac{z_i z_j e^2}{4\pi\epsilon_0 r_{ij}} + A_{ij} \exp\left(-\frac{r_{ij}}{\rho_{ij}}\right) - \frac{C_{ij}}{r_{ij}^6} \quad (1)$$

A Morse potential accounts for the covalent bond between anion and cation; see Eq. 2. In this equation r_{ij}^* is the covalent bond length. Coefficients D_{ij} and β_{ij} determine depth and shape of the potential.

$$U_{ij}(r_{ij}) = D_{ij} \{ \exp[-2\beta_{ij}(r_{ij} - r_{ij}^*)] - 2\exp[-\beta_{ij}(r_{ij} - r_{ij}^*)] \} \quad (2)$$

Two interatomic potentials have been compared in the calculations presented here. Coefficients of the first model, thereafter P1, are consistent with those published by Uchida et al. [17]. Ionicity of this potential is set to 0.565 and effective charges of plutonium and oxygen are set to +2.26 and -1.13, respectively. Values of the coefficients of P1 are reported in [12]. Coefficients of the second model, thereafter P2, are listed in Tab. 1. The effective charges of plutonium and oxygen are in this case set to +2.02 and -1.01, respectively. Compared to [12], P2 coefficients have been modified and refined aiming at improving, as discussed in previous section, the accuracy of linear thermal expansion predictions as well as at reducing the formation energy of OFP that is a key quantity of most recent models as recalled in the introduction.

Table 1: Coefficients of P2 potential

Pair (BMH)	A _{ij} (eV)	ρ _{ij} (Å)	C _{ij} (eV·Å ⁶)
O-O	334895.0	0.178	140.0
Pu-Pu	490000.0	0.250	0.0
Pu-O	4580.0	0.252	0.0
Pair (Morse)	D _{ij} (eV)	β _{ij} (Å ⁻¹)	r _{ij} [*] (Å)
Pu-O	0.30	2.	2.37

2.2 Modelling of heat capacity

Models for the heat capacity of PuO₂ usually employ three or more terms. In our case we consider the following terms: phonon c_{ph} , dilation c_d , and formation of defects c_{df} ; see Eq. 3 [11,18].

$$c_p = c_{ph} + c_d + c_{df} \quad (3)$$

The dilation term is shown in Eq. 4. In this equation α is the coefficient of volumetric thermal expansion, γ the Grüneisen constant, T the temperature.

$$c_d = \alpha\gamma c_{ph} T \quad (4)$$

Aiming at identifying a single term accounting for the increase of heat capacity at high temperature we have assumed that the correlation existing between the quantities determined in our calculations is resumed by Eq. 5. In this way we state that the scope of MD calculations is limited to the first two terms of Eq. 3 under the hypothesis that the third contribution c_{df} is modelled by means of the correlation proposed in [8].

$$c_p = c_{ph} \cdot (1 + \gamma\alpha T) \quad (5)$$

C_p and α have been evaluated with MD calculations in the NPT ensemble. The phonon term c_{ph} has been evaluated by means of MD calculations in the NVT ensemble. This

approach has therefore allowed us to determine through Eq. 5 the value of the Grüneisen constant that is now an output and not an initial assumption as in [12]. In turn, the determination of the Grüneisen constant allows us to evaluate the Bulk modulus of PuO₂ according to Eq. 6 [19].

$$B = \frac{c_p h \gamma}{\alpha \cdot V_m} \quad (6)$$

In Eq. 6 V_m stands for the molar volume. The other symbols have been presented in previous parts of the paper.

2.3 Details of calculations

Calculations in the NPT and NVT ensembles have been performed in the temperature domain 300-2900 K. In the low temperature domain (300-1500 K) calculations have been carried out every 100 K. From 1500 K up to 2900 K the interval between measurements has been reduced to 50 K. Additional calculations have been performed at 3000 K, 3100 K, 3200 K, 3300 K. The supercell used in calculations is composed of 40500 atoms arranged in a face-centered cubic lattice (*fcc*). The supercell has been constructed from the elementary cell that is composed of 12 atoms by replicating it 15x15x15 along the x , y , z orthogonal axes. Periodic boundary conditions have been applied. Energy minimization has been performed by means of a steepest descent algorithm. The Nose-Hoover thermostat/barostat has been used for equilibration of the system (30 ps) [13]. Quantities have been recorded in calculations with a time step of 1 fs and for an overall period of 30 ps.

3 RESULTS OF MD CALCULATIONS

3.1 Linear thermal expansion

The linear thermal expansion of plutonium dioxide has been calculated according to the values of lattice parameter determined in the NPT ensemble. Results are presented in Fig. 1 together with the experimental results on PuO₂ by Uchida et al. [17], the curve recommended for UO₂ by Martin [20], and the experimental measurements performed by Kato et al. on MOX fuel with a plutonium concentration of 48 mol% [21].

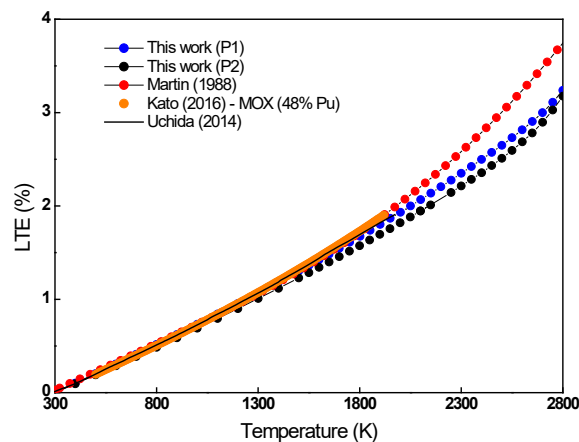


Figure 1: Linear thermal expansion as a function of temperature: comparison with the experimental results

Predictions of P1 are consistent with measurements and the curve recommended for PuO_2 [17]. This latter curve is not shown in Fig. 1 as above 1923 K it has been obtained by using an interatomic potential that is quite consistent with P1. Predictions of both potentials are in roughly good agreement, however, results of P2 underestimate P1 predictions that are quite consistent, as just mentioned, with the curve recommended for PuO_2 . However, compared to the P2 results presented in [12] a clear improvement has been achieved by using the coefficients listed in Tab. 1. In general, UO_2 , PuO_2 and MOX are in good agreement up to 2000 K, thereafter PuO_2 deviates from the recommendations of Martin [20]. No experimental results have been published in this temperature domain.

3.2 Grüneisen constant and Bulk modulus as a function of temperature

The Grüneisen constant has been calculated by means of Eq. 5. Results are presented in Fig. 2. The open literature reports following values: 2.30 [15], 1.62 [22] and 2.60 [23]. Both models predict values of the Grüneisen constant that are quite close to the results at RT presented in [15]. This quantity, after a slight decrease, shows to be roughly constant up to 2300-2500 K where a significant and steady increase is noticed. The increase is more pronounced for P2. The Bulk modulus as a function of temperature has been calculated by using Eq. 6 and results are presented in Fig. 2. Predictions of both potentials decrease with increasing temperature. In the intermediate part of the temperature domain, values of the Bulk modulus are nearly constant while at high temperature a significant recovery is seen especially for P2.

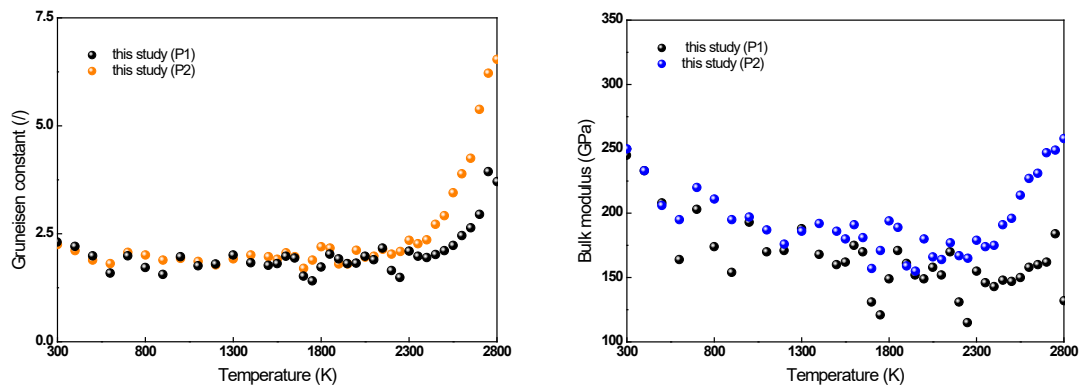


Figure 2: Grüneisen constant (left) and Bulk modulus (right) as a function of temperature

The elastic constants have been determined at 0 K according to the method proposed in [24]; see Tab. 2. In this case the Bulk modulus is in good agreement with [15] and in reasonable agreement with the values calculated by means of Eq. 6; see Fig. 2 (right). However, data available in the open literature and reported in Tab. 2, confirm a significant scatter so that deviations of our results could be still acceptable. A second interpretation of these results could address the fact that MD calculations below 500 K are less accurate as they do not account for quantum mechanical effects [25]. This has been noticed also for the heat capacity where an overestimation of data at 300 K has been confirmed. If we apply the same approach to the results on the Grüneisen constant we could suggest a value slightly lower than reported in [15].

Table 2: Elastic constants of plutonium dioxide

Elastic constants (GPa)	P1	P2	Reference data
Bulk modulus	206.30	225.20	200 [17], 225 [15], 218 [26], 178 [27]
Shear modulus	111.32	109.13	95 [15]
Young's modulus	283.04	281.67	249 [15]
Poisson's number (/)	0.27	0.29	0.319 [15]

3.3 Heat capacity at constant pressure and at constant volume

The heat capacity at constant pressure has been determined by means of MD calculations in the NPT ensemble according to the correlation presented in Eq. 7. In this equation H is the enthalpy in J/mol and T is the temperature in K.

$$c_p = \left(\frac{\partial(H-H_0)}{\partial T} \right)_p \quad (7)$$

The heat capacity at constant volume has been calculated in the NVT ensemble through the derivative of the total energy. The heat capacity at constant pressure (c_p) and constant volume (c_{ph}) are presented in Fig. 3. Curves recommended for UO_2 and PuO_2 are included for comparison [9]. Results of P2 are higher than P1 and closer to the recommended values in the high-temperature domain. The heat capacity at constant volume is rather flat with a tendency to increase approaching melting.

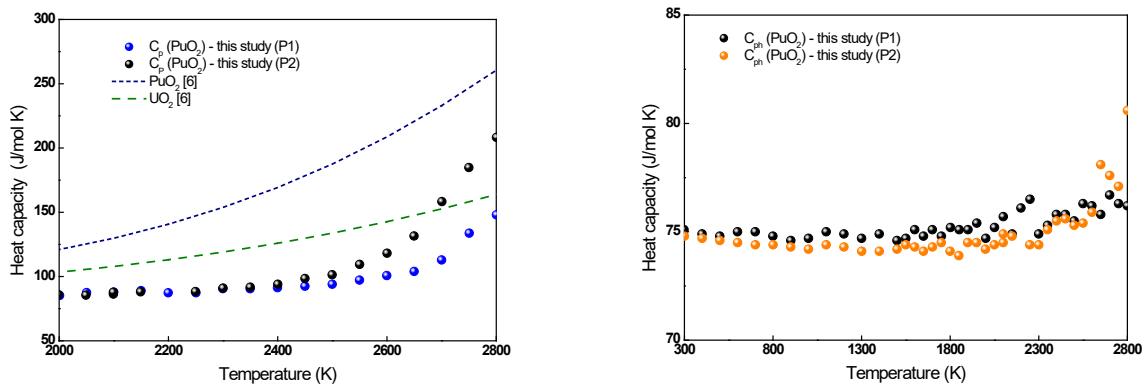


Figure 3: Heat capacity at constant pressure (left) and at constant volume (right) as a function of temperature

4 DISCUSSION

Results of MD calculations presented in this paper have been obtained by applying two BMH interatomic potentials: P1, taken as reference, and P2, that is an improved version of the model presented in [12]. Concerning the formation energy of OFP, evaluations carried out by applying the P1 potential have suggested a value of 9.28 eV. With regard to P2, this quantity has moved from 6.40 eV [12] to 5.73 eV. Concerning the thermal expansion of PuO_2 , even if some underestimation of P2 is noted, a significant improvement has been obtained compared to the results presented in [12]. Results on the Grüneisen constant show good agreement with recent measurements performed at room temperature [15]. With regard to the Bulk modulus.

we have observed an overestimation of the results published by Hirooka and Kato [15] if Eq. 6 is applied. A better agreement has been shown by using the approach presented in [24]. This could address also some inaccuracy of low temperature MD calculations as reported by other authors [25]. Nevertheless, both models agree on a markedly decrease of the Bulk modulus with increasing temperature. This result is consistent with the open literature up to the onset of the pre-melting transition, that, according to these results, introduces significant deviations between models' predictions. MD calculations clearly indicate that most of the excess heat capacity predicted by the recommended curve is due to clustering and configurational entropy of OFP defects. BMH potentials predict an increase of heat capacity beyond 2400 K that is about 85% of the melting temperature. Results of heat capacity do not show peaks that are usually attributed to the Bredig transition [28]. The presence of a pre-melting transition has been confirmed in some recent experimental measurements that are reported and discussed in [28]. Our results may confirm that the OFP formation energy is correlated with the increase noted in c_{ph} . In this view, we have highlighted that the distinction between pre-melting and melting is quite relevant and improvements are necessary for a sound and reliable evaluation of this issue. Classical MD calculations and the use of BMH potentials are capable of predicting only part of the recommended values of heat capacity. Therefore, it is confirmed the need for an additional term based, according to the indications of the literature, on the model proposed by Konings and Beneš. The OFP formation energy proposed by authors could be interpreted as an effective value that accounts for both disorder of anion sub-lattice and clustering of defects as discussed in our paper [12].

5 CONCLUSIONS

This paper presents MD calculations focused on the heat capacity of PuO_2 at high temperature. Moving from our previous results some issues concerning modelling of heat capacity, input value of the Grüneisen constant, and dimensional behaviour have been discussed in more detail leading to the definition of a new set of coefficients for the P2 potential. The evaluations performed on the Grüneisen constant and Bulk modulus showed to be in good agreement with data in the open literature especially in the temperature interval 600-2500 K. Compared to previous calculations, we have achieved a better agreement between P2 predictions and the linear thermal expansion curve recommended for PuO_2 and a lower value of the formation energy of OFP. New results confirm the presence of a pre-melting transition occurring at temperature higher than 85% of the melting temperature. In agreement with the open literature, a correlation between heat capacity and formation energy of OFP has been observed under pre-melting conditions. Overall, main conclusions of our previous analysis have been confirmed relying on a more robust and sound basis thanks to a revised approach that has been applied in the MD calculations presented in this paper.

REFERENCES

- [1] A.K. Sengupta, K.B. Khan, J. Panakkal, H.S. Kamath, S. Banerjee, "Evaluation of high plutonia (44% PuO_2) MOX as a fuel for fast breeder test reactor", *Journal of Nuclear Materials*, 385, 2009, pp. 173-177.
- [2] M. Kato, T. Matsumoto, "Thermal and Mechanical Properties of UO_2 and PuO_2 ", report NEA/NSC/R(2015)2, Nuclear Energy Agency, Paris, 2015, pp. 172-177.
- [3] M. Bober, G. Schumacher, D. Geithoff, "Plutonium redistribution in fast reactor mixed oxide fuel pins", *Journal of Nuclear Materials*, 47, 1973, pp. 187-197.

- [4] J.K. Fink, "Enthalpy and Heat Capacity of the Actinide Oxides", *International Journal of Thermophysics*, 3(2), 1982, pp. 165-200.
- [5] J.-M. Bonnerot, "Proprietes Thermiques des Oxydes Mixtes d'Uranium et de Plutonium", Ph.D. thesis, in report CEA-R-5450, CEA, Cadarache, France, 1988.
- [6] J.J. Carbajo, G.L. Yoder, S.G. Popov, V.K. Ivanov, "A review of the thermophysical properties of MOX and UO₂ fuels", *Journal of Nuclear Materials*, 299, 2001, pp. 181-198.
- [7] J.H. Harding, D.G. Martin, P.E. Potter, "Thermophysical and thermochemical properties of fast reactor materials", report EUR 12402 EN, Commission of the European Communities, Luxemburg, 1989.
- [8] R.J.M. Konings, O. Beneš, "The heat capacity of NpO₂ at high temperatures: The effect of oxygen Frenkel pair formation", *Journal of Physics and Chemistry of Solids*, 74(5), 2013, pp. 653-655.
- [9] R.J.M. Konings, O. Beneš, A. Kovács, D. Manara, D. Sedmidubsky, L. Gorokhov, V.S. Iorish, V. Yungman, E. Shenyavskaya, E. Osima, "The Thermodynamic Properties of the f-Elements and their Compounds. Part 2. The Lanthanide and Actinide Oxides", *Journal of Physical and Chemical Reference Data*, 43, 2014, p. 013101.
- [10] S.O. Válu, O. Beneš, D. Manara, R.J.M. Konings, M.W.D. Cooper, R.W. Grimes, C. Guéneau, "The high-temperature heat capacity of the (Th,U)O₂ and (U,Pu)O₂ solid solutions", *Journal of Nuclear Materials*, 484, 2017, pp. 1-6.
- [11] K. Kurosaki, K. Yamada, M. Uno, S. Yamanaka, K. Yamamoto, T. Namekawa, "Molecular dynamics study of mixed oxide fuel", *Journal of Nuclear Materials*, 294, 2001, pp. 160-167.
- [12] R. Calabrese, "The Heat Capacity of PuO₂ at High Temperature: Molecular Dynamics Calculations", *Journal of Nuclear Engineering and Radiation Science*, 2022, <https://doi.org/10.1115/1.4054941>.
- [13] S. Plimpton, "Fast Parallel Algorithms for Short-Range Molecular Dynamics", *Journal of Computational Physics*, 117, 1995, pp. 1-19.
- [14] ENEA, "High Performance Computing on CRESCO infrastructure: research activities and results 2019", Italian National Agency for New Technologies Energy and Sustainable Economic Development, Rome, 2019.
- [15] S. Hirooka, M. Kato, "Sound speeds in and mechanical properties of (U,Pu)O_{2-x}", *Journal of Nuclear Science and Technology*, 55(3), 2017, pp. 356-362.
- [16] K. Yamada, K. Kurosaki, M. Uno, S. Yamanaka, "Evaluation of thermal properties of mixed oxide fuel by molecular dynamics", *Journal of Alloys and Compounds*, 307, 2000, pp. 1-9.
- [17] T. Uchida, T. Sunaoshi, K. Konashi, M. Kato, "Thermal expansion of PuO₂", *Journal of Nuclear Materials*, 452, 2014, pp. 281-284.
- [18] H. Serizawa, Y. Arai, "An examination of the estimation method for the specific heat of TRU dioxides: evaluation with PuO₂", *Journal of Alloys and Compounds*, 312, 2000, pp. 257-264.

- [19] P. Tiwary, A. van de Walle, B. Jeon, N. Gronbech-Jensen, "Interatomic potentials for mixed oxide and advanced nuclear fuels", *Physical Review B*, 83, 2011, p. 094104.
- [20] D.G. Martin, "The thermal expansion of solid UO_2 and (U,Pu) mixed oxides - a review and recommendations", *Journal of Nuclear Materials*, 152, 1988, pp. 94–101.
- [21] M. Kato, Y. Ikusawa, T. Sunaoshi, A.T. Nelson, K.J. McClellan, "Thermal expansion measurement of (U,Pu) O_{2-x} in oxygen partial pressure-controlled atmosphere", *Journal of Nuclear Materials*, 469, 2016, pp. 223–227.
- [22] H. Serizawa, Y. Arai, Y. Suzuki, "Simultaneous determination of X-ray Debye temperature and Grüneisen constant for actinide dioxides: PuO_2 and ThO_2 ", *Journal of Nuclear Materials*, 280(1), 2000, pp. 99-105.
- [23] R.B. Jr Roof, "An experimental determination of the characteristic temperature for PuO_2 ", *Journal of Nuclear Materials*, 2(1), 1960, pp. 39–42.
- [24] <https://github.com/lammps/lammps/tree/master/examples/ELASTIC>.
- [25] S.I. Potashnikov, A.S. Boyarchenkov, K.A. Nekrasov, A.Ya. Kupryazhkin, "High-precision molecular dynamics simulation of UO_2 – PuO_2 : Pair potentials comparison in UO_2 ", *Journal of Nuclear Materials*, 419, 2011, pp. 217–225.
- [26] S. Li, R. Ahuja, B. Johansson, "High pressure theoretical studies of actinide oxides", *High Pressure Research*, 22, 2002, pp. 471-474.
- [27] M. Idiri, T. Le Bihan, S. Heathman, J. Rebizant, "Behavior of actinide oxides under pressure: UO_2 and ThO_2 ", *Physical Review B*, 70, 2004, p. 014113.
- [28] C. Takoukam-Takoundjou, E. Bourasseau, V. Lachet, "Study of thermodynamic properties of $\text{U}_{1-y}\text{Pu}_y\text{O}_2$ MOX fuel using classical molecular Monte Carlo simulations", *Journal of Nuclear Materials*, 534, 2020, p 152125.